CFD Letters

Journal homepage: https://semarakilmu.com.my/journals/index.php/CFD_Letters/index
ISSN: 2180-1363

Exact Analysis of Unsteady Convective Diffusion in Herschel-Bulkley Fluid Flow- Application to Catheterised Stenosed Artery

Siti Nurul Aifa Mohd Zainul Abidin[1], Nurul Aini Jaafar[1], Zuhaila Ismail[1,*]

[1] Department of Mathematical Sciences, Fakulti of Science, Universiti Teknologi Malaysia, 81310 Skudai, Johor, Malaysia

ARTICLE INFO

Article history:
Received 23 July 2022
Received in revised form 5 September 2022
Accepted 7 September 2022
Available online 10 November 2022

Keywords:
Blood flow; catheter; solute dispersion; Stenosis; Herschel-Bulkley fluid

ABSTRACT

One of the major causes of cardiovascular disease is atherosclerosis or stenosis. This study is designed to improve the current body of knowledge regarding the condition by inserting a long thin tube called a catheter to widen the narrow part in the artery. The study reviewed the effects of catheter radius, yield stress, and power law index on the velocity distribution, and transport coefficients of solute. A mathematical model is deployed to investigate the dispersion of solute in the flow of a Herschel-Bulkley (H-B) fluid in an annulus, whereas the dispersion process is studied using the generalised dispersion model (GDM) by solving the convective diffusion equation. Resultantly, the velocity reduces following an increase in the yield stress, catheter size, and power law index. Meanwhile, the dispersion coefficient exhibits a same behaviour as the aforementioned parameters ascend considerably. The dispersion coefficient alterations occurred rapidly for small values of time and became significantly constant following an increase in the time values. Conclusively, this study can be useful in dispersion of a drug to the affected artery where an abnormal plaque was formed.

1. Introduction

The transportation of solute dispersion process has been widely studied due to its extensive application in the field of chemical engineering, physiological fluid dynamics, biomedical engineering, environmental sciences, and pharmacology [1,2]. Studies on the dispersion of solute, such as drug, toxin, or nutrient, in blood flow through a narrow artery having a linear or constricted wall received much attention owing to its significant contribution in understanding the issues in biomedical engineering and cardiovascular mechanics [3-5]. Constriction in an artery occurs because of the accumulation of low-density lipoprotein (LDL) and other macromolecules along the inner lining of the arterial wall. The formation of such lesion or plaque started blocking the artery and reducing the normal blood flow, medically termed as atherosclerosis or stenosis. It is important for clinicians to analyse the rate of dispersion of an injected drug associated with intravenous drug delivery into an affected artery because of its therapeutic nature and also to measure the amount of drug in the system for better efficacy as well as the effectiveness of the delivery [6]. In this situation, a long thin

* *Corresponding author.*
E-mail address: zuhaila@utm.my

https://doi.org/10.37934/cfdl.14.11.7587

tube called a catheter is inserted into the veins to refine the flow. The use of catheters is of immense importance and has become a standard tool for diagnosis and treatment in modern medicine [7]. The catheter is carefully guided to the location at which stenosis occurs and the balloon is then inflated to fracture the fatty deposits and widen the narrowed part of the artery.

Catheterized arteries are now extensively used in medical science to measure various physiological flow characteristics as well as to diagnose and treat various arterial diseases. Numerous researchers have recently evaluated the blood flow in an annulus employed in a catheterised stenosed artery [8-10]. However, these studies did not consider the mass transfer that governs the flow of mass transport in the systemic circulation. The convective diffusion equation controls the mass transfer to the bloodstream [11]. A method known as the generalised dispersion model (GDM) was proposed by Gill and Sankarasubramanian [12] to generate an exact solution of the convective diffusion equation, which is applicable at all times.

Hence, based on the existing literature, there is a lack of studies on the problem of unsteady solute dispersion in blood flow by considering the H-B fluid model in an overlapping catheterised stenosed artery using the GDM. This study extends the works by Sankar and Hemalatha [13] and Abbas *et al*. [14] by investigating the rheological behaviour of blood flow in an overlapping stenosed artery. The investigation of solute dispersion in a non-Newtonian fluid is crucial to yield realistic results that better represent physical problems. This study aims to investigate how reactive solute disperse in the solvent is influenced by physical parameters such as catheter radius, yield stress, and power law index. Specifically, the contributions of the study are twofold, firstly to evaluate the effects of reactive species in an overlapping catheterised stenosed artery using GDM that was only addressed individually in previous studies, and secondly to analyse the rheological behaviour of non-Newtonian fluid in a catheterised stenosed artery.

2. Mathematical Formulation

A catheter is inserted into an artery coaxially, and the artery takes the form of a rigid circular tube. Radius of the circular tube is R_0 and radius of the catheter is given as kR_0, $k < 1$. Consider a steady, axially symmetrical, laminar, and fully developed uni-directional flow of blood in the axial direction portrayed as a viscous incompressible non-Newtonian fluid. Herschel-Bulkley (H-B) fluid model is employed to illustrate the blood flow. The entrance, endpoint and distinctive wall effects of the artery can be disregarded given the sufficient length of the arterial segment.

2.1 Governing Equations

A cylindrical polar coordinate $(\bar{r}, \bar{\theta}, \bar{z})$ is used in the study where $\bar{r}$ and $\bar{z}$ denote the radial and axial coordinates and $\bar{\theta}$ is the azimuthal angle. The fluid velocity in $\bar{r}$ direction is ignored as its magnitude is negligibly small and only accounts in a $\bar{z}$ direction. Thus, $\bar{u}_{\bar{r}} = \bar{u}_{\bar{\theta}} = 0$ [15]. Since the pressure gradient is a function of $\bar{z}$ only and independent of $\bar{r}$ and $\bar{\theta}$, thus $d\bar{p}/d\bar{z}$ is constant, hence, the momentum equation can be simplified as

$$\frac{d\bar{p}}{d\bar{z}} = -\frac{1}{\bar{r}}\frac{d}{d\bar{r}}\left(\bar{r}\,\bar{\tau}\right), \quad \bar{k} \le \bar{r} \le \bar{R}\left(\bar{z}\right), \tag{1}$$

where the constant pressure, shear stress, catheter radius and radius of stenosed artery are represented as $\bar{p}, \bar{\tau}, \bar{k}$ and $\bar{R}(\bar{z})$, respectively. The following equation presents the constitutive equation of H-B fluid

$$\eta_{HB}\frac{\partial \bar{u}}{\partial \bar{r}}=\begin{cases}\left|\bar{\tau}\right|^{n}\left(1-\dfrac{n\bar{\tau}_{y}}{\left|\bar{\tau}\right|}\right)^{n}, & \text{if } \left|\bar{\tau}\right|\geq\bar{\tau}_{y} \text{ and } \dfrac{\partial \bar{u}}{\partial \bar{r}}>0,\\ -\left|\bar{\tau}\right|^{n}\left(1-\dfrac{n\bar{\tau}_{y}}{\left|\bar{\tau}\right|}\right)^{n}, & \text{if } \left|\bar{\tau}\right|\geq\bar{\tau}_{y} \text{ and } \dfrac{\partial \bar{u}}{\partial \bar{r}}<0,\\ 0, & \text{if } \left|\bar{\tau}\right|<\bar{\tau}_{y}.\end{cases} \tag{2}$$

where $\bar{u}, \bar{\tau}_{\bar{y}}$ and n is the axial velocity, yield stress, and power law index, respectively. Meanwhile, the H-B fluid viscosity coefficient is represented by η_{HB} with dimension $(ML^{-1}T^{-2})^{n}T$. The unknown parameters, velocity $\bar{u}$ and shear stress $\bar{\tau}$, can be solved using Eqs. (1) and (2) based on the no-slip boundary conditions for the catheter wall and artery presented below

$$\begin{aligned}&\bar{u}=0 \quad \text{when } \bar{r}=\bar{k},\\ &\bar{u}=0 \quad \text{when } \bar{r}=\bar{R}\left(\bar{z}\right).\end{aligned} \tag{3}$$

2.2 Non-dimensionalisation

Introducing the following dimensionless variables

$$\begin{aligned}&C=\frac{\bar{C}}{\bar{C}_{0}},u=\frac{\bar{u}}{u_{0}},u_{m}=\frac{\bar{u}_{m}}{u_{0}},r=\frac{\bar{r}}{R_{0}},R(z)=\frac{\bar{R}(\bar{z})}{R_{0}},z=\frac{\bar{z}}{R_{0}},\\ &\tau=\frac{\bar{\tau}}{(p_{0}R_{0}/2)},\theta=\frac{\bar{\tau}_{y}}{(p_{0}R_{0}/2)},l_{0}=\frac{\bar{l}_{0}}{R_{0}},\delta=\frac{\bar{\delta}}{R_{0}},k=\frac{\bar{k}}{R_{0}},\end{aligned} \tag{4}$$

where C is the solute concentration, u is the velocity, u_m is the average velocity, $u_0=\frac{R_0^{n+1}{p_0}^{n}}{2^{n}\eta_{HB}}$ is the centreline velocity, r is the radial distance, $R(z)$ is the radius of the stenotic artery, z is the axial distance, τ is the shear stress, θ is the yield stress, l_0 is the stenosis length, δ is the stenosis height, k is the catheter radius and $\eta_{HB}=\mu\left(\frac{p_0R_0}{2}\right)^{n-1}$, where μ is the viscosity coefficient for a Newtonian fluid.

2.3 Geometry of Stenosis

The geometry of the artery in the dimensionless form can be written as Layek *et al.,* [16] and ZainulAbidin *et al*., [17]

$$R(z)=\begin{cases}1-\dfrac{3\delta}{2{l_0}^{4}}\left[11(z-d){l_0}^{3}-47(z-d)^{2}{l_0}^{2}+72(z-d)^{3}l_0-36(z-d)^{4}\right], & d\leq z\leq d+l_0,\\ 1, & \text{Otherwise,}\end{cases} \tag{5}$$

where δ is the maximum stenosis height occurs at $d + l_0/3$ and $d + 2l_0/3$, d is the distance of the stenosis from the inlet, and *L* is the length of the artery. The geometry of a catheterised artery with an overlapping stenosis under consideration is shown in Figure 1.

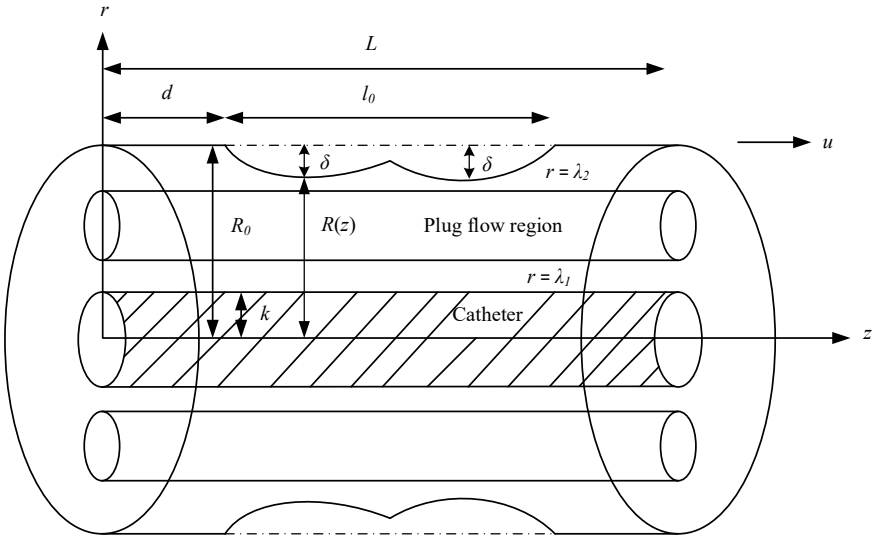

Fig. 1. The geometry of catheterised artery with an overlapping stenosis

2.4 Mass Transport

The transport of a reactive solute in the bloodstream in dimensionless form is governed by the convection-diffusion equation [18], which is expressed as

$$\frac{\partial C}{\partial t} + u\frac{\partial C}{\partial z} = \left(\frac{1}{r}\frac{\partial}{\partial r}\left(r\frac{\partial}{\partial r}\right) + \frac{1}{Pe^2}\frac{\partial^2}{\partial z^2}\right)C, \tag{6}$$

where *Pe* is the Peclet number, *t* is the dispersion time, D_m is molecular diffusivity of the solute which is assumed as constant.

2.5 Method of Solution

The momentum Eq. (1) in dimensionless form can be stated as

$$p_s = \frac{1}{2r}\frac{d}{dr}(r\tau), \quad k \le r \le R(z), \tag{7}$$

where p_s is the dimensionless pressure gradient in steady state. The constitutive Eq. (2) in dimensionless form is

$$\frac{\partial u}{\partial r}=\begin{cases}|\tau|^n\left(1-\dfrac{n\theta}{|\tau|}\right), & \text{for } |\tau|\geq\theta \text{ and } \dfrac{\partial u}{\partial r}>0,\\ -|\tau|^n\left(1-\dfrac{n\theta}{|\tau|}\right), & \text{for } |\tau|\geq\theta \text{ and } \dfrac{\partial u}{\partial r}<0,\\ 0, & \text{for } |\tau|<\theta.\end{cases} \tag{8}$$

Integrating Eq. (7) with respect to *r* yields

$$\tau=p_s r+\frac{C}{r}, \tag{9}$$

where C is the constant of integration. Referring to Eq. (8), there are three different flow regions for $k\leq r\leq R(z)$, in which the central core region has a constant velocity and forms the plug flow region. Flow in this plug flow region is not sheared which means blood streamlines are moving at constant velocity because the shear stress is lesser than yield stress. The fluid (blood) will not flow at this region rather it is transported by the fluid particles present in the nearby shear flow region as a solid mass with a constant velocity. For mathematical representation, the plug flow region can be described by $\lambda_1\leq r\leq\lambda_2$, where $k\leq\lambda_1$ and $\lambda_2\leq R(z)$. λ_1 and λ_2 are unknown constants to be identified. The three regions are depicted as in Figure 1. From the continuity of the shear stress along the plug flow region boundary, we have

$$\begin{aligned}-\tau&=\tau_y \text{ when } r=\lambda_1,\\ \tau&=\tau_y \text{ when } r=\lambda_2.\end{aligned} \tag{10}$$

Using condition (10) in Eq. (9), the unknown constant C is evaluated in terms of λ_1 and λ_2 as

$$C=-p_s\lambda^2, \tag{11}$$

where

$$\lambda^2=\lambda_1\lambda_2. \tag{12}$$

Substitution of Eq. (11) in Eq. (9) delineates the shear stress as

$$\tau=\frac{p_s}{r}\left(r^2-\lambda^2\right). \tag{13}$$

Using Eq. (13) and condition (10) yields

$$\lambda_2-\lambda_1=\frac{\theta}{p_s}=\varsigma_A, \tag{14}$$

where ς_A is the width of the plug core region. Velocity expressions for the three regions can be found using Eqs. (13) and (8) as below

$$u^{+}(r)=p_s{}^{n}\left[\int_k^r\left(\frac{\lambda^2-r^2}{r}\right)^n dr-n\varsigma_A\int_k^r\left(\frac{\lambda^2-r^2}{r}\right)^{n-1} dr\right],\ \text{when } k\le r\le\lambda_1, \tag{15}$$

$$u_p=u^{+}(\lambda_1)=u^{++}(\lambda_2)=\text{constant},\ \text{when } \lambda_1\le r\le\lambda_2, \tag{16}$$

$$u^{++}(r)=p_s{}^{n}\left[\int_r^{R(z)}\left(\frac{r^2-\lambda^2}{r}\right)^n dr-n\varsigma_A\int_r^{R(z)}\left(\frac{r^2-\lambda^2}{r}\right)^{n-1} dr\right],\ \text{when } \lambda_2\le r\le R(z), \tag{17}$$

where $u^{+}(r), u_p$ and $u^{++}(r)$ represent the shear flow region from $k\le r\le\lambda_1, \lambda_1\le r\le\lambda_2$ and $\lambda_2\le r\le R(z)$, respectively. Absence of yield stress $(\theta=0)$ will result to $\varsigma_A=0$, where both Eqs. (15) and (17) will result to velocity field in the catheterised artery for power law fluid, a finding that is in line with Kapur [19]. To ensure continuous velocity distribution for the entire flow field, below condition needs to be fulfilled

$$u^{+}(r=\lambda_1)=u_p=u^{++}(r=\lambda_2). \tag{18}$$

This gives

$$\int_k^{\lambda_1}\left(\frac{\lambda^2-r^2}{r}\right)^n dr-\int_{\lambda_2}^{R(z)}\left(\frac{r^2-\lambda^2}{r}\right)^n dr-n\varsigma_A\left[\int_k^{\lambda_1}\left(\frac{\lambda^2-r^2}{r}\right)^{n-1} dr-\int_{\lambda_2}^{R(z)}\left(\frac{r^2-\lambda^2}{r}\right)^{n-1} dr\right]=0. \tag{19}$$

Using Eqs. (12) and (14), Eq. (19) can be simplified into integral equation in λ_1 as below

$$\begin{aligned}&\int_k^{\lambda_1}\left(\frac{\lambda_1(\lambda_1+\varsigma_A)-r^2}{r}\right)^n dr-\int_{\lambda_1+\varsigma_A}^{R(z)}\left(\frac{r^2-\lambda_1(\lambda_1+\varsigma_A)}{r}\right)^n dr\\&-n\varsigma_A\left[\int_k^{\lambda_1}\left(\frac{\lambda_1(\lambda_1+\varsigma_A)-r^2}{r}\right)^{n-1} dr-\int_{\lambda_1+\varsigma_A}^{R(z)}\left(\frac{r^2-\lambda_1(\lambda_1+\varsigma_A)}{r}\right)^{n-1} dr\right]=0.\end{aligned} \tag{20}$$

λ_1 in Eq. (20) is solved numerically using Regula-Falsi method whereas the integrals is evaluated via Simpson's 3/8 rule. Once λ_1 is known, λ_2 can be determined using Eq. (14). According to Gill and Sankarasubramanian [12], the solution of Eq. (6) is computed as a series expansion and is displayed as

$$C(r,z,t)=C_m(z_1,t)+\sum_{i=R(z)}^{\infty} f_i(r,t)\frac{\partial^i C_m(z_1,t)}{\partial z_1^i}, \tag{21}$$

where C_m is the mean concentration, f_i is dispersion function and a new axial coordinate moving with the average velocity is $z_1 = z - u_m t$. The distribution of C_m is diffusive as the time starts and thus, the GDM as appropriate functions of time *t* is given as

$$\frac{\partial C_m}{\partial t} = \sum_{i=1}^{\infty} K_i(t) \frac{\partial^i C_m}{\partial z_1^i}(z_1, t), \tag{22}$$

where $K_i(t)$ is the dispersion coefficient. Substituting Eq. (21) into Eq. (6) and using Eq. (22) yields the series expansion. By equating the coefficients of $\partial^i C_m / \partial z_1^i$ and let $f_1(r,t) = f_{1s}(r) + f_{1t}(r,t)$, where f_{1s} is the steady-state and f_{1t} is the unsteady state, the variable separation method and Bessel function can be used to solve the transient state, $f_{1t}(r,t)$ of the dispersion function subject to the conditions $f_{1t}(r,0) = -f_{1s}(r)$ and $\partial f_{1t}/\partial r = 0$. The solution $f_{1t}(r,t)$ is numerically computed using Simpson's 3/8 rule and presented as

$$f_{1t}(r,t) = \sum_{m=1}^{\infty} A_m B_0 e^{-\left(\lambda_m^2 + \gamma^2\right)t}, \tag{23}$$

where

$$A_m = -\frac{\int_k^{R(z)} B_0 \, f_{1s}(r) r \, dr}{\int_k^{R(z)} B_0^2 \, r \, dr}, \tag{24}$$

$$B_0 = J_1(\lambda_m k) Y_0(\lambda_m r) - Y_1(\lambda_m k) J_0(\lambda_m r) \tag{25}$$

and the factors λ_m are the solutions of the equation

$$J_1(\lambda_m R(z)) Y_1(\lambda_m k) - J_1(\lambda_m k) Y_1(\lambda_m R(z)) = 0, \tag{26}$$

with J_0, J_1, Y_0 and Y_1 indicate the Bessel functions for first and second kind of order zero and one, respectively. By substituting Eq. (21) into the transport equation Eq. (6) yield a partial differential equation for mean concentration as below

$$\begin{aligned} &\frac{\partial C_m}{\partial t} + (u - u_m)\frac{\partial C_m}{\partial z_1^1} - \frac{1}{Pe^2}\frac{\partial^2 C_m}{\partial z_1^2} + \sum_{j=1}^{\infty}\left(\left(\frac{\partial f_j}{\partial t} - \frac{1}{r}\frac{\partial}{\partial r}\left(r\frac{\partial f_j}{\partial r}\right)\right)\frac{\partial^j C_m}{\partial z_1^j}\right. \\ &\left. + (u - u_m) f_j \frac{\partial^{j+1} C_m}{\partial z_1^{j+1}} - \frac{1}{Pe^2} f_j \frac{\partial^{j+2} C_m}{\partial z_1^{j+2}} + f_j \frac{\partial^{j+1} C_m}{\partial z_1^{j+1} \partial t}\right) = 0. \end{aligned} \tag{27}$$

Substituting Eq. (22) in Eq. (27) and rearranging terms yields

$$\left[K_1(t)+(u-u_m)+\frac{\partial f_1}{\partial t}-\frac{1}{r}\frac{\partial}{\partial r}\left(r\frac{\partial f_1}{\partial r}\right)\right]\frac{\partial C_m}{\partial z_1^1}+\left[-\frac{1}{Pe^2}+(u-u_m)f_1+f_1K_1(t)+K_2(t)\right.$$
$$+\frac{\partial f_2}{\partial t}-\frac{1}{r}\frac{\partial}{\partial r}\left(r\frac{\partial f_2}{\partial r}\right)\Big]\frac{\partial^2 C_m}{\partial z_1^2}+\sum_{j=1}^{\infty}\Big[-\frac{1}{Pe^2}f_j+(u-u_m)f_{j+1}+K_{j+2}(t)+\frac{\partial f_{j+2}}{\partial t} \tag{28}$$
$$\left.-\frac{1}{r}\frac{\partial}{\partial r}\left(r\frac{\partial f_{j+2}}{\partial r}\right)+\sum_{i=1}^{j+1}K_i(t)f_{j+2-i}\right]\frac{\partial^{j+2}C_m}{\partial z_1^{j+2}}=0.$$

For $j=1,2,\ldots.$, we equalize $\partial^i C_m/\partial z_1^j$ to zero to obtain the infinite system of partial differential equations as below

$$\frac{\partial f_1}{\partial t}-\frac{1}{r}\frac{\partial}{\partial r}\left(r\frac{\partial f_1}{\partial r}\right)_1+u-u_m+K_1(t)=0, \tag{29}$$

$$\frac{\partial f_2}{\partial t}-\frac{1}{r}\frac{\partial}{\partial r}\left(r\frac{\partial f_2}{\partial r}\right)+\left[u-u_m+K_1(t)\right]f_1+K_2(t)-\frac{1}{Pe^2}=0, \tag{30}$$

$$\frac{\partial f_{i+2}}{\partial t}-\frac{1}{r}\frac{\partial}{\partial r}\left(r\frac{\partial f_{j+2}}{\partial r}\right)+\left[u-u_m+K_1(t)\right]f_{j+1}+\left[K_2(t)-\frac{1}{Pe^2}\right]f_j+\sum_{i=1}^{j+1}K_i(t)f_{j+2-i}=0, \tag{31}$$

for $j=1,2,\ldots.$ with $f_0=1$.

By multiplying Eqs.(29), (30) and (31) with r followed by integrating the result from *k* to $R(z)$ imply

$$K_1(t)=-\frac{2}{1-k^2}\int_k^{R(z)}(u-u_m)\,r\,dr=0, \tag{32}$$

$$K_2(t)=\frac{1}{Pe^2}-\frac{2}{1-k^2}\int_k^{R(z)}f_1\,u\,r\,dr, \tag{33}$$

$$K_{j+2}(t)=-\frac{2}{1-k^2}\int_k^{R(z)}f_{j+1}\,u\,r\,dr,\quad j=1,2,\ldots.. \tag{34}$$

The dispersion coefficient $K_2(t)$ is an indicator to measure the effectiveness of the solute dispersion in the blood flow. Ramana *et al*. [20] and Dash *et al*. [21] evaluated the overall reduction in solute dispersion due to the fluid yield stress at a constant pressure gradient by subtracting $1/Pe^2$ and multiplying 192 to Eq. (33) resulting to

$$192\left(K_2(t)-\frac{1}{Pe^2}\right)=-\frac{2}{1-k^2}\int_k^{R(z)}f_1\,u\,r\,dr. \tag{35}$$

3. Results and Discussion

3.1 Validation

The effect of varying catheter radius, power law index, and yield stress on the velocity profile and dispersion coefficient of solute is analysed, with the following range of parameters: k: $0.1-0.3, \theta$: $0.1-0.3$, and n: $0.75-2$ [13,22]. The results and data were generated for both comparison and validation purposes using the Mathematica software. Figures 2 (a), 2 (b) and 2 (c) confirmed that the steady dispersion function f_{1s}, unsteady dispersion function f_{1t} and dispersion function f_1 of solute obtained in this study is comparable with the findings of Jaafar [23]. For validation purposes, k and δ was set to zero while the geometry of the stenosed artery, *R*(*z*) was set to one to resemble fluid without stenosis and catheter.

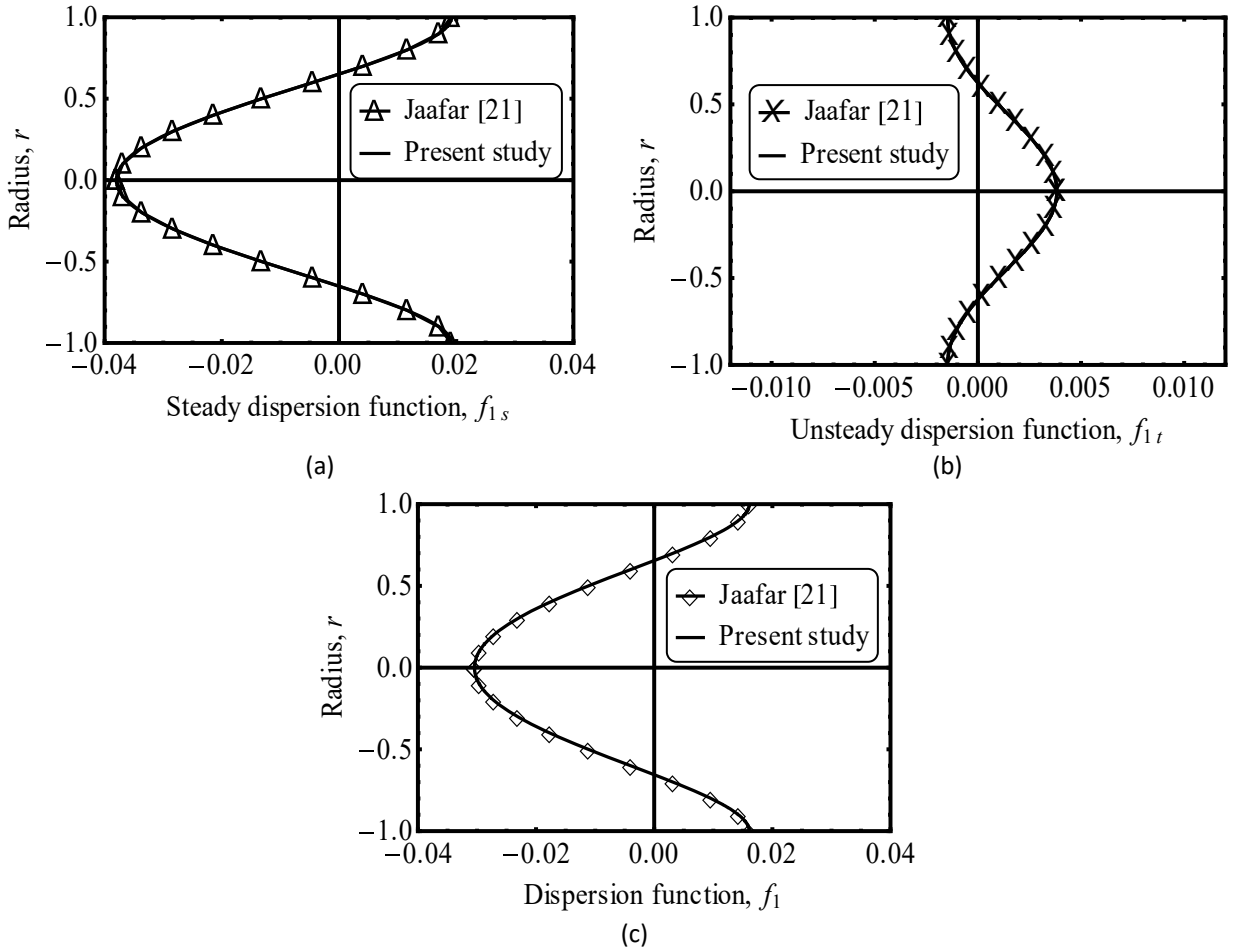

Fig. 2. The parameters are fixed at $n = 0.95, \beta = 0.1, R(z) = 1, \delta = 0$, $k = 0$ and $\theta = 0.1$ (a) steady dispersion function f_{1s}, (b) unsteady dispersion function f_{1t} with $t = 0.1$ and (c) dispersion function f_1 with $t = 0.1$

3.2 Velocity

It is crucial to ensure drug is quickly and efficiently dispersed as soon as possible in order to cure relevant disease. In this case, blood velocity will play a vital role in this direction as it influences the convection and dispersion coefficient [24]. Figure 3 (a) illustrates the variation in velocity distribution with different catheter radius when $p_s = 1, \theta = 0.1, n = 0.95, l_0 = 3, d = 2, z = 4$ and $\delta = 0.01$. In the case of constant yield stress, increase in catheter radius will result to decrease in

axial velocity because of the reduction in annular flow in the area between catheter wall and arterial wall.

From the velocity distribution recorded by various fluids in Figure 3 (b), we can see that highest velocity is recorded by power law fluid compare with fluids having yield stress; for example, for $n = 0.95$, power law fluid velocity is higher than Newtonian fluid when $n = 1, \theta = 0$. However, for specific values of k and θ, improvement in n results to lessen velocity when $p_s = 1, l_0 = 3, d = 2, z = 4$ and $\delta = 0.01$. Comparing between H-B fluid and Bingham fluid under a similar yield stress, it is shown that as power law index increases from $n = 0.95$ to $n = 1$, the axial velocity slightly decreases. Bessonov *et al.* [25] reported that the erythrocyte concentration is higher near the axis, whereas the platelets are concentrated near the wall. Sankar and Hemalatha [13] stated that results of velocity distribution discovered by Dash *et al*. [21] for Casson fluid are significantly lesser compared to H-B fluid.

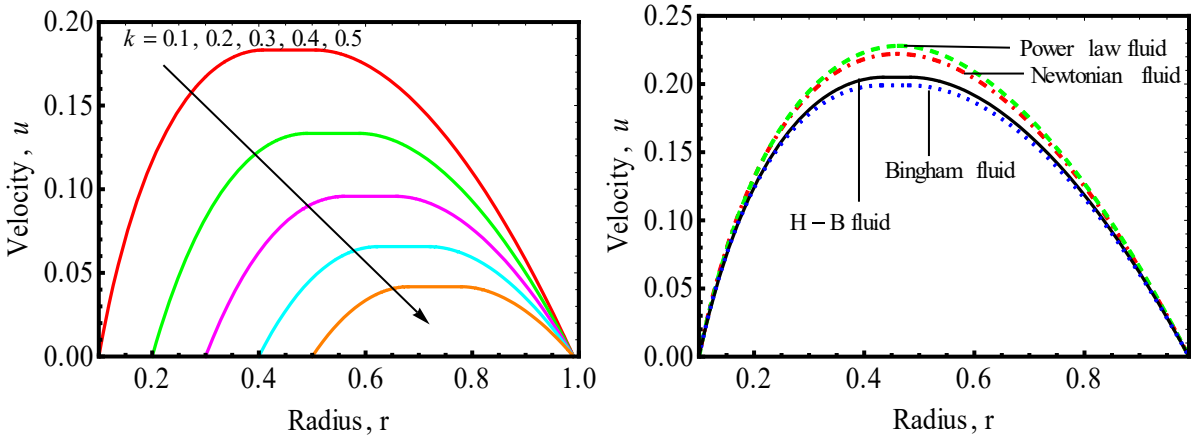

Fig. 3. Variation of the velocity distribution when $p_s = 1, \delta = 0.01,\ l_0 = 3, d = 2$ and $z = 4$ for (a) different catheter radius k with $n = 0.95$ and $\theta = 0.1$ (b) different fluids with $k = 0.1$

3.3 Dispersion Coefficient

Dispersion coefficient $K_2(t)$ explains the overall dispersion process in terms of simple diffusion process as a function of time. The results when $k = 0$ and $\theta = 0$ reduce to those of [12]. Figure 4 (a) illustrates the variation of dispersion coefficient over time t for various catheter size *k* when $n = 0.95, p_s = 1, \theta = 0.1, \delta = 0.01, l_0 = 3, d = 2$ and $z = 4$. It is observed that with an increase in the catheter size from $k = 0.1$,0.15, 0.2, 0.25 to 0.3, the dispersion coeffficient reduces significantly. As the catheter size increase, the annular gap between stenosed arterial wall and catheter wall decreases because reduction in annular gap hampers dispersion process. The same behaviour was also noticed by Rao and Desikachar [26] for a Newtonian fluid.

Figure 4 (b) shows the variation of dispersion coefficient over time t for various power law index *n* when $p_s = 1, \theta = 0.1, k = 0.1, \delta = 0.01, l_0 = 3, d = 2$ and $z = 4$. The dispersion coefficient of the solute diminish as the power law index *n* increases. As mentioned by Hussain *et al.* [27], the power-law index represents the apparent whole blood viscosity. Power law index plays an important role to control viscosity and velocity of a fluid. Physically, the viscosity of the fluid increases as the power-law index increases, hence blood travels faster along the axial distance. When the viscosity increases in the blood flow, the solute movement becomes slower, and hence, the dispersion coefficient decreases.

Figure 4 (c) elucidates the variation of dispersion coefficient over time t for various yield stress θ when $p_s = 1, n = 0.95, k = 0.1, l_0 = 3, d = 2, z = 4$ and $\delta = 0.01$. The dispersion coefficient decreases significantly as θ increases from $\theta = 0, 0.05, 0.1, 0.15$ and 0.2. At $t = 0.4$, the dispersion coefficient reaches a steady-state of diffusion when $K_2(t) = 0.083, 0.0080, 0.0070, 0.0065$ and 0.0063, respectively with an increase in θ. The dispersion coefficient rises rapidly from $t = 0$ to 0.2, then slowly from $t = 0.2$ to 0.4 and becomes almost constant from $t = 0.4$ to 0.5. It can be seen that the dispersion coefficient $K_2(t)$ changes quickly for short time scale but it does not change much for large time scale. Specifically for Newtonian fluid $(\theta = 0, n = 1)$, it attains steady-state at time t of around 0.5. Due to yield stress, time recorded will be lower because yield stress corresponds to the non-Newtonian nature of the fluid where improvement in yield stress equals to higher blood viscosity. Apart from that, yield stress is also related to the width of the plug region where improvement in said width will improve yield stress as portrayed in Eq. (14).

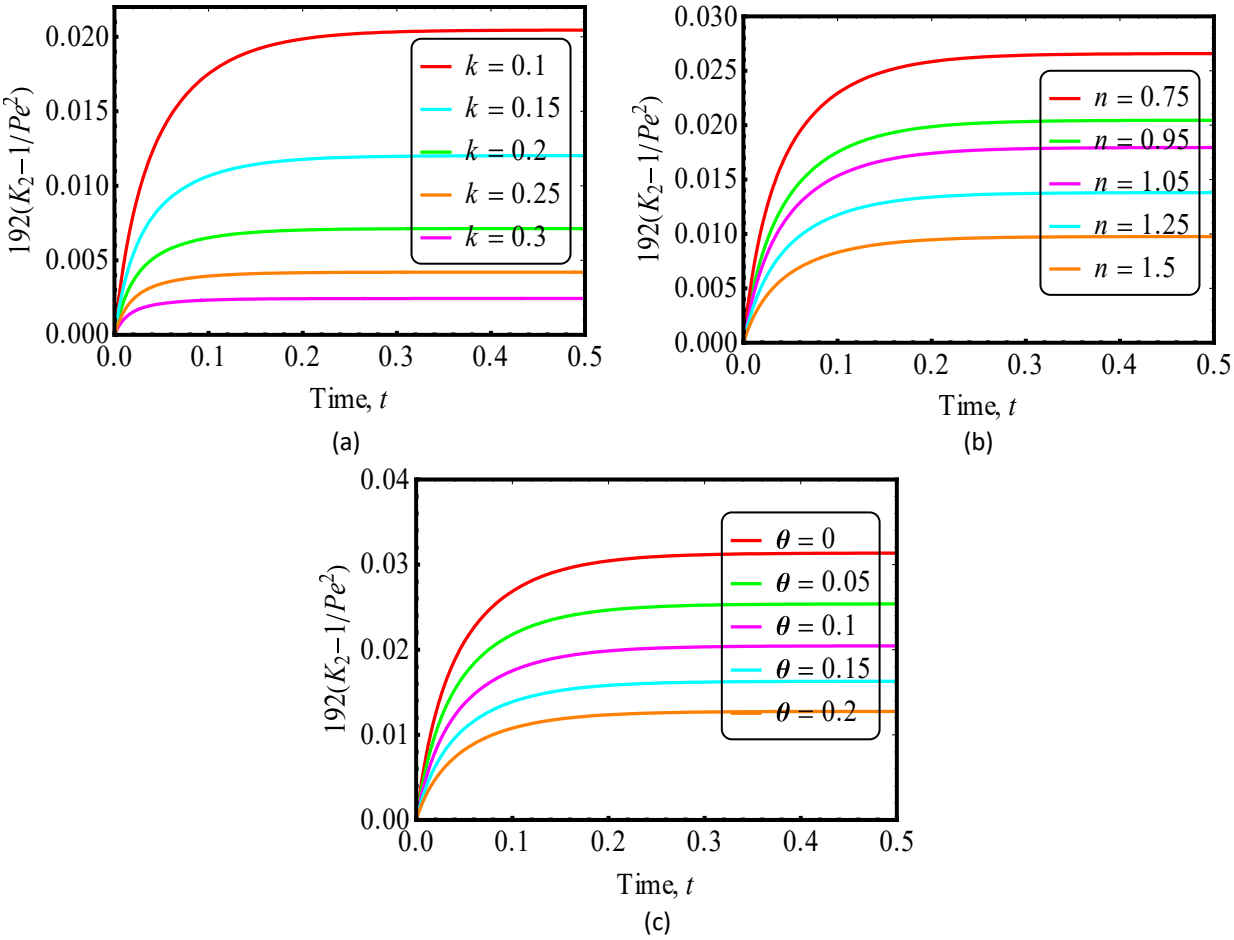

Fig. 4. Variation of dispersion coefficient K_2 over time t when $p_s = 1, \delta = 0.01,\ l_0 = 3, d = 2$ and $z = 4$ for (a) different catheter radius k with $n = 0.95$ and $\theta = 0.1$ (b) different power law index with $k = 0.1$ and $\theta = 0.1$ (c) different yield stress with $n = 0.95$ and $k = 0.1$

4. Conclusion

The present study investigated the influence of catheter radius, power law index, and yield stress of the fluid on the solute dispersion process in the cardiovascular system. The important findings are outlined below:

- Upon inserting a catheter into the lumen of the artery, the presence of a plug flow region results in the production of two yield plane locations;
- The velocity reduces following an increase in the yield stress, catheter size, and power law index. The dispersion coefficient exhibits a same behaviour as the aforementioned parameters ascend considerably;
- The dispersion coefficient exhibits two distinctive behaviours which are linear and non-linear behaviour.

Since this model did not consider the flow pulsatility and the porosity of the arterial tissue, hence, future researchers are recommended to extend this study.

Acknowledgement
The authors would like to acknowledge Ministry of Higher Education and Research Management Centre, Universiti Teknologi Malaysia for the financial support through vote numbers 09G88 (UTMShine Grant), 5F255 (FRGS Grant) and 21H48 (UTMFR Grant).

References

[1] Das, Prosanjit, and Prashanta Kumar Mandal. "Solute dispersion in Casson fluid flow through a stenosed artery with absorptive wall." *Zeitschrift für angewandte Mathematik und Physik* 71, no. 3 (2020): 1-24. https://doi.org/10.1007/s00033-020-01322-8

[2] Ndenda, J. P., S. Shaw, and J. B. H. Njagarah. "Solute dispersion of drug carrier during magnetic drug targeting for blood flow through a microvessel." *Journal of Applied Physics* 130, no. 2 (2021): 024701. https://doi.org/10.1063/5.0053645

[3] Roy, Ashis Kumar, and O. Anwar Bég. "Mathematical modelling of unsteady solute dispersion in two-fluid (micropolar-Newtonian) blood flow with bulk reaction." *International Communications in Heat and Mass Transfer* 122 (2021): 105169. https://doi.org/10.1016/j.icheatmasstransfer.2021.105169

[4] Debnath, Sudip, Weiquan Jiang, Mingyang Guan, and Guoqian Chen. "Effect of ring-source release on dispersion process in Poiseuille flow with wall absorption." *Physics of Fluids* 34, no. 2 (2022): 027106. https://doi.org/10.1063/5.0077957

[5] Jaafar, Nurul Aini, Siti NurulAifa Mohd ZainulAbidin, Zuhaila Ismail, and Ahmad Qushairi Mohamad. "Mathematical Analysis of Unsteady Solute Dispersion with Chemical Reaction Through a Stenosed Artery." *Journal of Advanced Research in Fluid Mechanics and Thermal Sciences* 86, no. 2 (2021): 56-73. https://doi.org/10.37934/arfmts.86.2.5673

[6] Das, Prosanjit, Sarifuddin, Jyotirmoy Rana, and Prashanta Kumar Mandal. "Solute dispersion in transient Casson fluid flow through stenotic tube with exchange between phases." *Physics of Fluids* 33, no. 6 (2021): 061907. https://doi.org/10.1063/5.0052770

[7] Srivastava, V. P., and Rati Rastogi. "Blood flow through a stenosed catheterized artery: Effects of hematocrit and stenosis shape." *Computers & mathematics with applications* 59, no. 4 (2010): 1377-1385. https://doi.org/10.1016/j.camwa.2009.12.007

[8] Rathore, Surabhi, and D. Srikanth. "Mathematical study of transport phenomena of blood nanofluid in a diseased artery subject to catheterization." *Indian Journal of Physics* 96, no. 7 (2022): 1929-1942. https://doi.org/10.1007/s12648-021-02166-2

[9] Tripathi, Jayati, B. Vasu, O. Anwar Bég, Rama Subba Reddy Gorla, and Peri K. Kameswaran. "Computational simulation of rheological blood flow containing hybrid nanoparticles in an inclined catheterized artery with stenotic, aneurysmal and slip effects." *Computers in Biology and Medicine* 139 (2021): 105009. https://doi.org/10.1016/j.compbiomed.2021.105009

[10] Zidan, A. M., L. B. McCash, Salman Akhtar, Anber Saleem, Alibek Issakhov, and Sohail Nadeem. "Entropy generation for the blood flow in an artery with multiple stenosis having a catheter." *Alexandria Engineering Journal* 60, no. 6 (2021): 5741-5748. https://doi.org/10.1016/j.aej.2021.04.058

[11] Sarifuddin. "CFD modelling of Casson fluid flow and mass transport through atherosclerotic vessels." *Differ Equ Dyn Syst* (2020). https://doi.org/10.1007/s12591-020-00522-y

[12] Gill, W. N., and R. Sankarasubramanian. "Exact analysis of unsteady convective diffusion." *Proceedings of the Royal Society of London. A. Mathematical and Physical Sciences* 316, no. 1526 (1970): 341-350. https://doi.org/10.1098/rspa.1970.0083

[13] Sankar, D. S., and K. Hemalatha. "A non-Newtonian fluid flow model for blood flow through a catheterized artery—steady flow." *Applied mathematical modelling* 31, no. 9 (2007): 1847-1864. https://doi.org/10.1016/j.apm.2006.06.009
[14] Abbas, Z., B. Iftikhar, M. S. Shabbir, M. Alghamdi, and J. Iqbal. "Numerical treatment of slip velocity and catheterization on the gravity flow of non-Newtonian fluid model through a uniform blood vessel." *Physica Scripta* 95, no. 5 (2020): 055006. https://doi.org/10.1088/1402-4896/ab6da2
[15] Swarup, S. (2000). *Chapter 5 - Fluid Dynamics.* Page 622-633.
[16] Layek, G. C., S. Mukhopadhyay, and Rama Subba Reddy Gorla. "Unsteady viscous flow with variable viscosity in a vascular tube with an overlapping constriction." *International journal of engineering science* 47, no. 5-6 (2009): 649-659. https://doi.org/10.1016/j.ijengsci.2009.01.011
[17] ZainulAbidin, Siti Nurulaifa Mohd, Zuhaila Ismail, and Nurul Aini Jaafar. "Mathematical Modeling of Unsteady Solute Dispersion in Bingham Fluid Model of Blood Flow Through an Overlapping Stenosed Artery." *Journal of Advanced Research in Fluid Mechanics and Thermal Sciences* 87, no. 3 (2021): 134-147. https://doi.org/10.37934/arfmts.87.3.134147
[18] Roy, Ashis Kumar, and O. Anwar Bég. "Asymptotic study of unsteady mass transfer through a rigid artery with multiple irregular stenoses." *Applied Mathematics and Computation* 410 (2021): 126485. https://doi.org/10.1016/j.amc.2021.126485
[19] Kapur, J. N. (1985). *Chapter 7 - Mathematical Models in Biology and Medicine.* Page 455-480.
[20] Ramana, B., G. Sarojamma, B. Vishali, and P. Nagarani. "Dispersion of a solute in a Herschel–Bulkley fluid flowing in a conduit." *Journal of Experimental Sciences* 3, no. 2 (2012).
[21] Dash, R. K., G. Jayaraman, and K. N. Mehta. "Shear augmented dispersion of a solute in a Casson fluid flowing in a conduit." *Annals of Biomedical Engineering* 28, no. 4 (2000): 373-385. https://doi.org/10.1114/1.287
[22] Abidin, Siti Nurul Aifa Mohd Zainul, Nurul Aini Jaafar, and Zuhaila Ismail. "Herschel-Bulkley Model of Blood Flow through a Stenosed Artery with the Effect of Chemical Reaction on Solute Dispersion." *Malaysian Journal of Fundamental and Applied Sciences* 17, no. 4 (2021): 457-474. https://doi.org/10.11113/mjfas.v17n4.2144
[23] Jaafar, Nurul Aini. "Mathematical Analysis of Herschel-Bulkley Fluid Model for Solute Dispersion in Blood Flow Through Narrow Conduits." PhD diss., PhD thesis, Universiti Sains Malaysia, 2017.
[24] Roy, Ashis Kumar, and Sachin Shaw. "Shear augmented microvascular solute transport with a two-phase model: Application in nanoparticle assisted drug delivery." *Physics of Fluids* 33, no. 3 (2021): 031904. https://doi.org/10.1063/5.0035754
[25] Bessonov, Nikolay, Adélia Sequeira, Sergey Simakov, Yu Vassilevskii, and Vitaly Volpert. "Methods of blood flow modelling." *Mathematical modelling of natural phenomena* 11, no. 1 (2016): 1-25. https://doi.org/10.1051/mmnp/201611101
[26] Ramachandra Rao, A., and K. S. Deshikachar. "An exact analysis of unsteady convective diffusion in an annular pipe." *ZAMM-Journal of Applied Mathematics and Mechanics/Zeitschrift für Angewandte Mathematik und Mechanik* 67, no. 3 (1987): 189-195. https://doi.org/10.1002/zamm.19870670315
[27] Hussain, Mohammad A., Subir Kar, and Ram R. Puniyani. "Relationship between power law coefficients and major blood constituents affecting the whole blood viscosity." *Journal of Biosciences* 24, no. 3 (1999): 329-337. https://doi.org/10.1007/BF02941247